

<https://doi.org/10.1038/s43247-024-01486-5>

Hot rings on Io observed by Juno/JIRAM

Check for updates

Alessandro Mura¹✉, Federico Tosi¹, Francesca Zambon¹, Rosaly M. C. Lopes², Peter J. Mougins-Mark³, Heidi Becker², Gianrico Filacchione¹, Alessandra Migliorini¹, Candice J. Hansen⁴, Alberto Adriani¹, Francesca Altieri¹, Scott Bolton⁵, Andrea Cicchetti¹, Elisa Di Mico¹, Davide Grassi¹, Raffaella Noschese¹, Alessandro Moirano¹, Madeline Pettine⁶, Giuseppe Piccioni¹, Christina Plainaki⁷, Julie Rathbun⁶, Roberto Sordini¹ & Giuseppe Sindoni⁷

It has been thought that Io's many paterae may contain lava lakes, but observations by NASA's Galileo spacecraft at sufficiently high resolution were limited to a few locations, such as Loki Patera. Data acquired by NASA's Juno mission in May 2023 reveal a common set of thermal characteristics for at least ten paterae on Io, with bright (hot) "thermal rings" around the perimeter of their floors. Loki, Surt, Fuchi, Amaterasu, Mulungu, Chors, and Dazhbog Patera, and four unnamed paterae, all show the same pattern of surface temperature. This new Juno/JIRAM data suggests that hot rings around paterae are a common phenomenon, and that they are indicative of active lava lakes. All the investigated paterae lack recent lava flows on their flanks, suggesting that at the time of observations, the level of the lake was not high enough to overflow the rim. These observations provide insight about the characteristics of paterae's activity, which may involve either central upwelling of magma, or up-and-down "piston-like" vertical motion of the lake surface. Tidal forces, which are extreme at Io, could play a role as well. Future observations from Juno, particularly during the closest flybys, may indicate which mechanism is more plausible.

The innermost Galilean moon of Jupiter, Io, is by far the most volcanically active body in the Solar System and is the only one besides Earth where active silicate volcanism has been observed^{1,2}. Io has a few large lava flows; however, the most common type of volcanic feature on Io is the "patera", which is a depression like a terrestrial caldera³; on Io, however, paterae can be much larger than on Earth (up to 200 km for Loki). To date, a large number (>250) of active volcanic features have been identified⁴⁻⁷. The composition of Ionian lavas has not been directly determined but, based on estimated values of lava temperatures, it has been inferred that the lavas are likely basaltic or potentially ultramafic in nature⁸⁻¹¹.

The paterae on Io have been interpreted to contain active lava based on both their morphological and thermal characteristics as observed by the NASA Galileo mission in 1995–2002. Studies based on Galileo infrared data revealed that the thermal expression of several hot volcanic features on Io is confined within paterae, and a few of them show greater thermal emission near the patera walls¹², which could indicate these are more likely lava lakes than lava flows. However, the available Galileo data show only a few examples of such increase of emission near the patera walls. Furthermore, the exact nature of the subsurface "plumbing system" feeding these lava lakes is unknown as different models imply different magma supply rates and, thus, heat flow¹³. Within an individual patera, Galileo data¹² and recent

Juno infrared images and spectra^{6,14}, show that the fraction of surface that is hot and emitting is not large, indicating that higher spatial resolution is needed to reveal these features.

In this report, we use data from the Juno spacecraft collected in May 2023 to analyze the temperature distribution within several active volcanic centers and what this implies for the possible eruption mechanisms.

Results

In May 2023, the Juno spacecraft performed a flyby of Io at ~35,000 km above its surface. The spacecraft orientation allowed Juno's Jovian InfraRed Auroral Mapper (JIRAM) to observe the moon for six hours. JIRAM is an infrared imaging spectrometer¹⁵, and during this encounter it collected 400 images of Io at ~3.5 μm (L-band) and ~4.8 μm (M-band) at a spatial resolution down to ~9 km/pixel (performance and details of the instrument are reported in the Supplementary Methods). A mosaic of the images in the M-band at the highest resolution available shows an abundance of active volcanic features (Fig. 1).

The JIRAM data reveal a common set of thermal characteristics for at least ten patera, with bright "thermal rings" around the perimeter of their floors. Loki, Surt, Fuchi, Amaterasu, Mulungu, Chors, and Dazhbog paterae, two unnamed paterae (here referred to as UP1 and UP2), and two other

¹Istituto Nazionale di Astrofisica—Istituto di Astrofisica e Planetologia Spaziali, Rome, Italy. ²Jet Propulsion Laboratory, California Institute of Technology, Pasadena, CA, USA. ³Hawaii Institute Geophysics and Planetology, Honolulu, HI, USA. ⁴Planetary Science Institute, Tucson, AZ, USA. ⁵Southwest Research Institute, San Antonio, TX, USA. ⁶Cornell University, Ithaca, NY, USA. ⁷Agenzia Spaziale Italiana, Rome, Italy. ✉e-mail: alessandro.mura@inaf.it

Fig. 1 | Mosaic map of M-band radiance from Io. The best spatial resolution M-band images have been composed to obtain a mosaic map of Io radiance; the spatial resolution is from 30 km/pixel (median) down to 9 km/pixel (best). White rectangles envelope the lava rings discussed in the study (L for Loki, A for Amaterasu, U for Unnamed UP1, M for Mulungu, C for Chors, D for Dazhbog, B for UP2 close to Bulicame Regio, S for Surt and F for Fuchi). The white contour lines mark the locations where the nominal spatial resolution is 10, 15, or 20 km/pixel. The red segments on the right indicate the length of 100 km at different latitudes. The red arrows indicate two small additional possible features. The projection of the map is a Miller cylindrical projection.

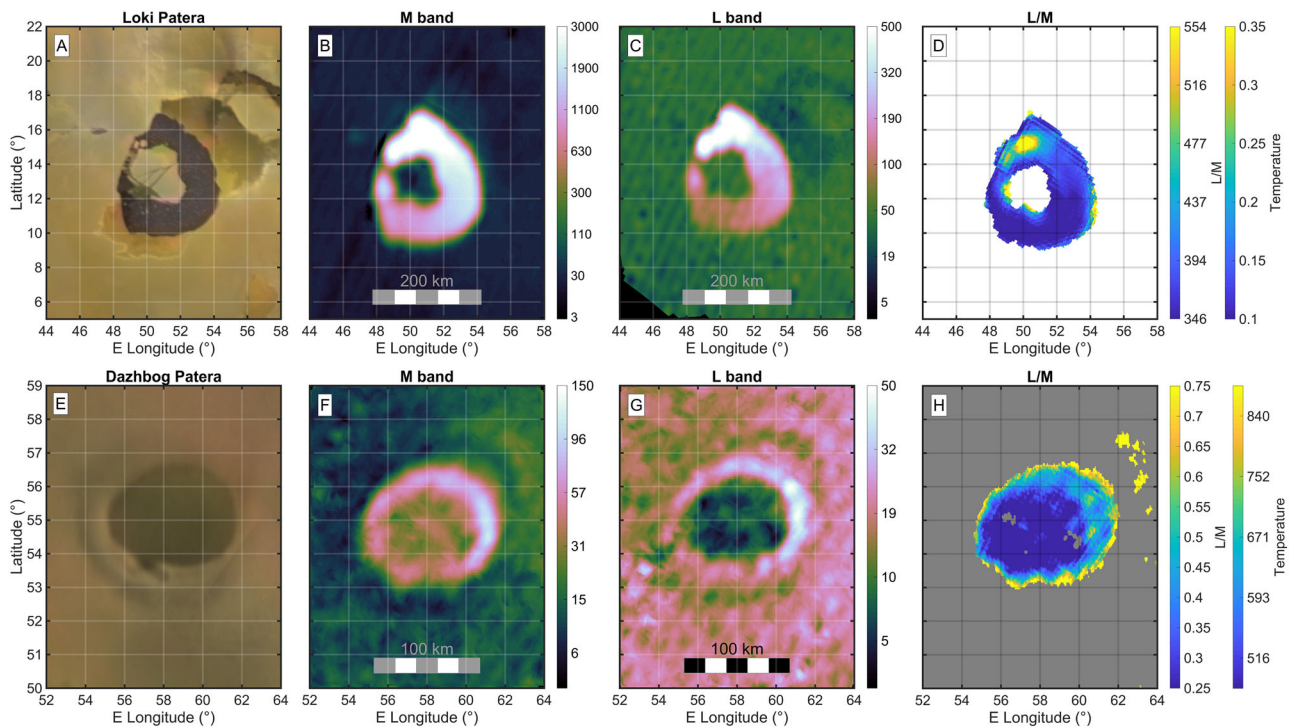
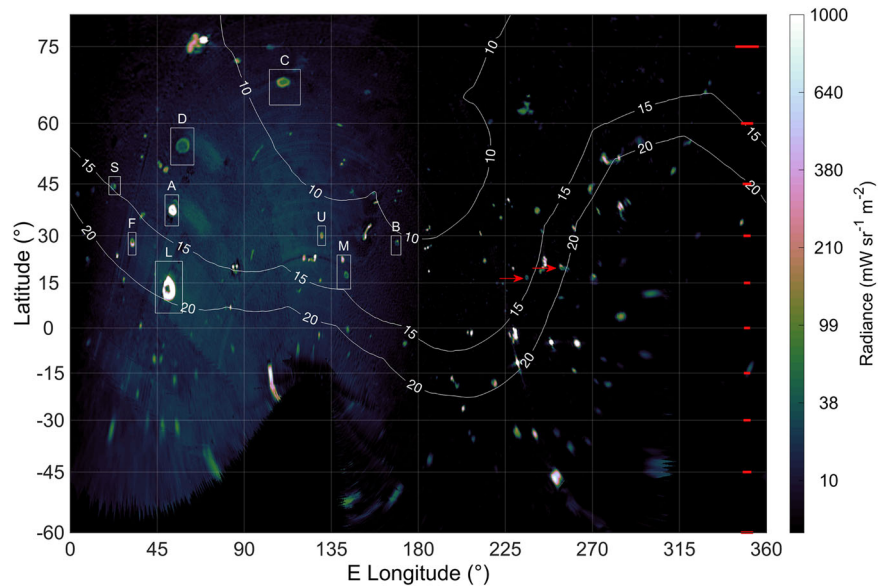


Fig. 2 | Visible maps, infrared radiance maps and temperature maps for Loki Patera and Dazhbog Patera. Top panels (A–D): Loki Patera. A USGS reference image; B M-band (4.5–5 μm) radiance map; C L-band (3.3 to 3.6 μm) radiance map (band radiance is integrated by the bandpass filter and it is in $\text{mW sr}^{-1} \text{m}^{-2}$); D L/M

ratio, and an estimation of the temperature (see Supplementary Fig. S11); gray region indicates where the signal is too low to calculate a significant ratio. Bottom panels (E–H): same for Dazhbog Patera.

potential additional paterae (not discussed further because the spatial resolution is poor), all show the same pattern of surface temperatures.

The Galileo NIMS instrument detected enhanced thermal emission at the edges of Loki Patera and Emakong Patera, and tentatively (due to lower resolution, ~ 8 km/pixel) at Tupan Patera, leading to the interpretation that these paterae contained lava lakes¹². Loki, the largest volcanic depression on Io, displays an abruptly infrared-dark central island^{2,16}. Galileo infrared data showed higher thermal emission at the edge of the patera and also against the central island¹². In Fig. 2, a visible-wavelength image of Loki from the Galileo Solid-State Imaging/Voyager

Color Merged Global Mosaic¹⁷, which combined the best images of Io from both missions, is compared to the same region as observed by JIRAM in the M and L filters and to the JIRAM L/M ratio, which can be used to obtain an approximate estimation of the blackbody temperature (see Methods). The estimated temperature has a peak of about 550 K in the northern part of the ring. Comparing JIRAM data of Loki to those from Galileo¹², including the visible images and the temperature map, shows that the patera surface has retained its size and shape, including its central island, over the last 25 years, despite frequent or perhaps constant activity⁷.

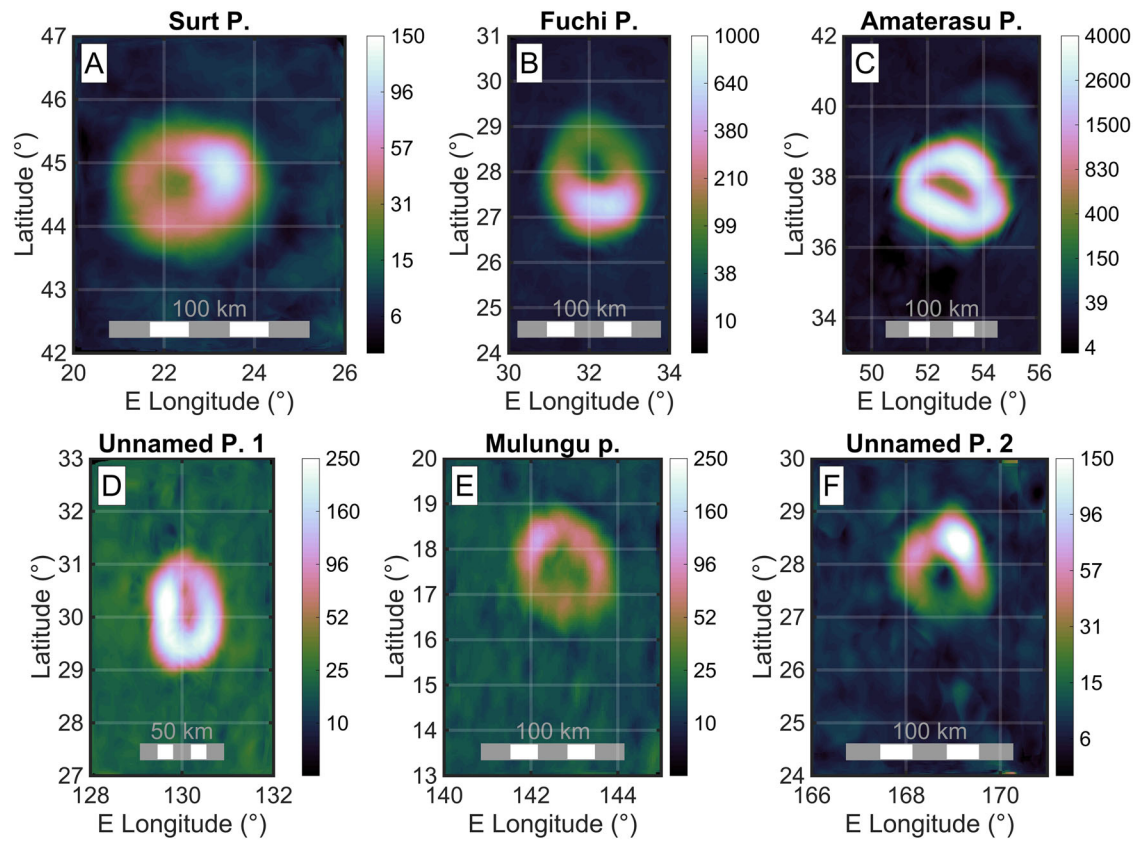


Fig. 3 | Infrared radiance maps for six different paterae showing lava rings. A Surt Patera; B Fuchi Patera; C Amaterasu Patera; D unnamed patera UP1; E Mulungu Patera; F unnamed patera (UP2) close to Bulicame Regio. The images show the band radiance in the M bandpass filter. Color scales are different from image to image, units are always $\text{mW sr}^{-1} \text{m}^{-2}$.

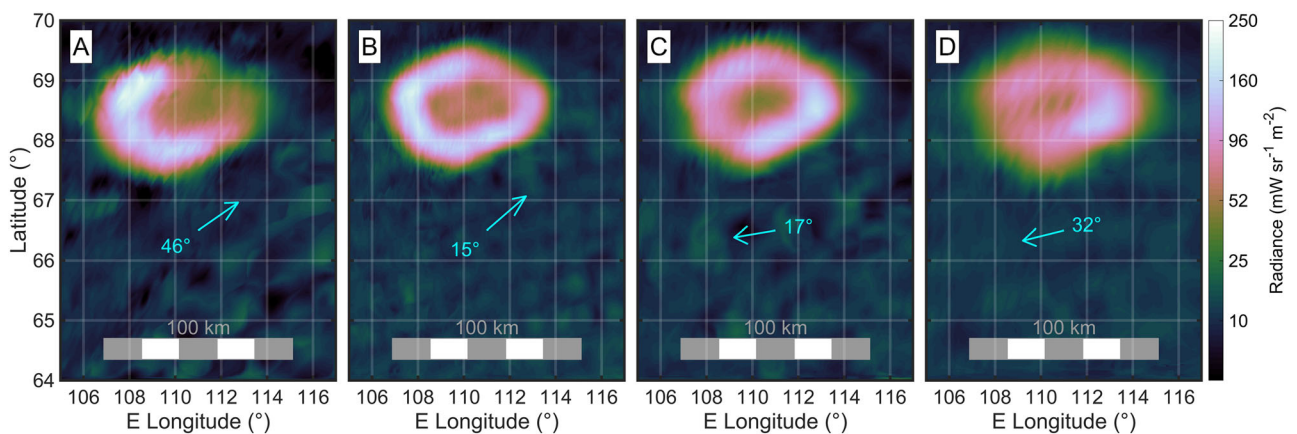


Fig. 4 | Infrared radiance maps of Chors Patera from different vantage points. Four M-band radiance maps of Chors Patera have been taken from different vantage points, the four acquisitions started respectively at 02:59:30 (A), at 03:09:38 (B), at 03:19:45 (C) and at 03:48:33 (D) on May 16th, 2023 (see Supplementary Methods). The cyan arrows indicate the direction of the sub-spacecraft point, and the cyan number is the emission angle at the time of the image acquisition.

In comparison, a similar set of images for Dazhbog Patera (Fig. 2) reveals a nearly perfectly circular shape without any hint of an island in the visible-wavelength images, and with maximum radiance intensity to the east. From the L/M ratio (see Supplementary Methods) we infer that the average temperature at the spatial resolution of JIRAM is nearly 900 K. Seven other examples of lava rings with no island have been observed in JIRAM data, namely Surt, Fuchi, Amaterasu, Mulungu Paterae, an unnamed patera (“UP1”, which it is close to JR159 in ref. 6 at 30°N, 130°E), an unnamed patera south of Bulicame Regio (“UP2” at 28°N, 169°E) (these six are shown in Fig. 3), and Chors Patera (Figs. 4 and 5). In all cases, the

external borders of the thermal rings are coaligned with the visible walls of the patera in the Galileo + Voyager global color mosaic¹⁷.

Supplementary Figs. S1–S7 show details of comparisons of the visible and IR maps (M band) of the other paterae included in this study. It is evident that the external borders of the hot rings are aligned with the visible walls of the paterae. We calculate the intensity of the M-band radiance along a segment across the ring, and we estimate the full-width half maximum (FWHM), which is assumed to be the apparent annular width of the ring (i.e., the difference between the outer and inner radii). It turns out that the FWHM is 20 km for Surt, 23 km for Fuchi, 23 km for Amaterasu, 11 km for

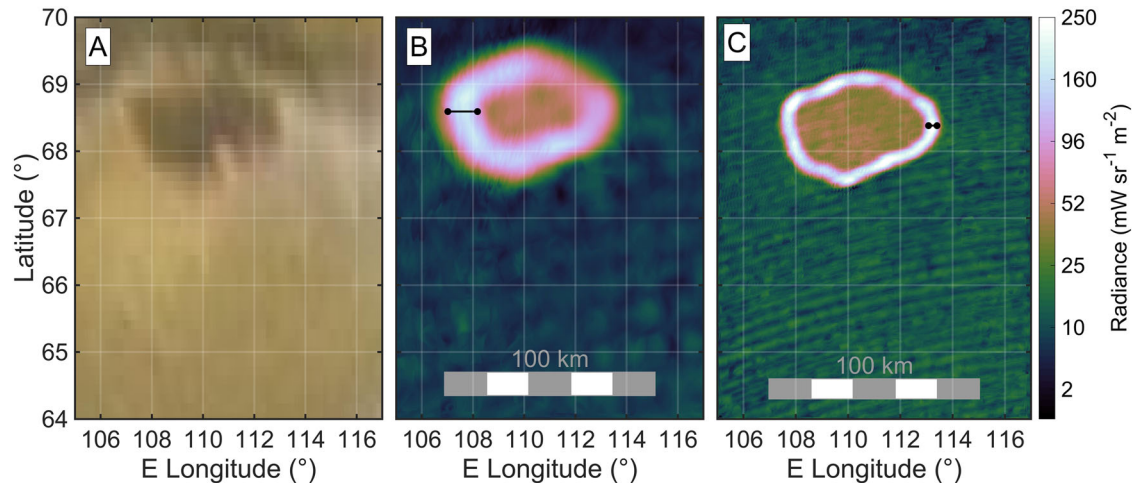


Fig. 5 | Visible map and infrared radiance maps for Chors Patera. **A** Chors Patera in the visible. **B** M-band image acquired on May 16th, 2023 (resolution: ~10 km/pixel). **C** same, for data acquired on October 15th, 2023 (resolution: 3 km/pixel,

maximum radiance is $300 \text{ mW sr}^{-1} \text{ m}^{-2}$). The black segments represent the FWHM of the ring annular width.

the unnamed patera UP1, 13 km for Mulungu, 13 km for the unnamed patera UP2, 13 km for Chors, and 16 km for Dazhbog. These values are represented by black segments in Fig. 5 and in Supplementary Figs. S1–S7.

These values are presumably much larger than the actual annular width, because these features are sub-pixel. To estimate the actual annular width, we made the following calculation. The emissivity of lava increases as temperature decreases¹⁸, ranging from 0.6 to 0.95; a blackbody with a temperature of ~500 K and emissivity of 0.6 emits a radiance of $\sim 50 \text{ W sr}^{-1} \text{ m}^{-2}$ in the 4.5–5.0 μm range, and one with a temperature of ~900 K and emissivity of 0.95 emits a radiance of $\sim 500 \text{ W sr}^{-1} \text{ m}^{-2}$ in the same range. Among these two cases, 500 K is a conservative value, since the temperature retrieval of Loki still shows a higher value in the region where lava is supposed to emerge (in agreement with the value of 570 K found for Loki¹²); the value of 900 K is chosen in agreement with that shown by Dazhbog Patera (see Fig. 2).

Hence, an expected band radiance of $50 \text{ W sr}^{-1} \text{ m}^{-2}$ is a very conservative lower limit, which we compare with the peak intensity of the band radiance. We then estimate the filling factor of the pixels with a simple proportion. As a result, the values we find for the actual annular width are upper limits; using the value of $500 \text{ W sr}^{-1} \text{ m}^{-2}$ will result in estimated annular widths that are 10 times lower. For example, Surt (Fig. 3, panel A) has a peak radiance of $150 \text{ mW sr}^{-1} \text{ m}^{-2}$, that is ~300 times smaller than the value of $50 \text{ W sr}^{-1} \text{ m}^{-2}$ estimated above; the filling factor is 1/300 and the estimated annular width is 20 km/300, that is ~60 m. For the other paterae we find the following values: 500 m for Fuchi, 1.5 km for Amaterasu, 60 m for the unnamed patera UP1, 30 m for Mulungu, 40 m for the unnamed patera UP2, 60 m for Chors, and 50 m for Dazhbog Patera. A more recent image (October 15, 2023, Fig. 5C) from a closer flyby of Io (13,000 km) shows again Chors Patera at better spatial resolution (~3 km). In this case, the apparent annular width is 3 km and, thanks to the better spatial resolution, the estimated upper limit for the actual annular can be lowered to 20 m. It is worth noting that the inner part of the patera (which we suggest is covered by crust, see next section) has a uniform radiance ($40 \text{ mW sr}^{-1} \text{ m}^{-2}$), which accounts for only 25% of the total M-band emitted power (1 GW). The average radiance of Chors Patera was $90 \text{ mW sr}^{-1} \text{ m}^{-2}$ for the first observation (May 2023) and $90 \text{ mW sr}^{-1} \text{ m}^{-2}$ for the second one (October 2023).

Figure 4 shows the dependence of the observed radiance as a function of the observation point for four different observations of Chors Patera. It is evident that the morphology of the lava ring, although obviously remaining unchanged in all four observations, shows that the location of maximum brightness is strongly dependent on the observer's viewpoint. The maximum brightness is always on the opposite side of the observer, which can be

explained by assuming that the patera floor is substantially lower (perhaps by tens or hundreds of meters) than the surrounding terrain, and that the lava ring always occupies the region adjacent to the patera's edges and is partially covered by the patera's wall, which is expected to be quite steep, perhaps nearly vertical. Indeed, the use of shadow calculations, such as the estimations for Chaac Patera³, demonstrated that these walls can reach heights up to 900 m.

Supplementary Figs. S8–S10 show a composition of images comparing Dazhbog, unnamed patera UP1 and unnamed patera UP2 as seen from different vantage points (for other paterae, data for such analysis is not available). It is evident that an effect similar to that seen in Fig. 4 also shows up for Dazhbog and the unnamed patera UP1. On the other hand, the unnamed patera UP2 does not show such an effect (or at least, it is not evident), but UP2 may be (see Fig. S6) a lake with a central island, so that the location of the maximum may be independent from the vantage point, as in the case of Loki.

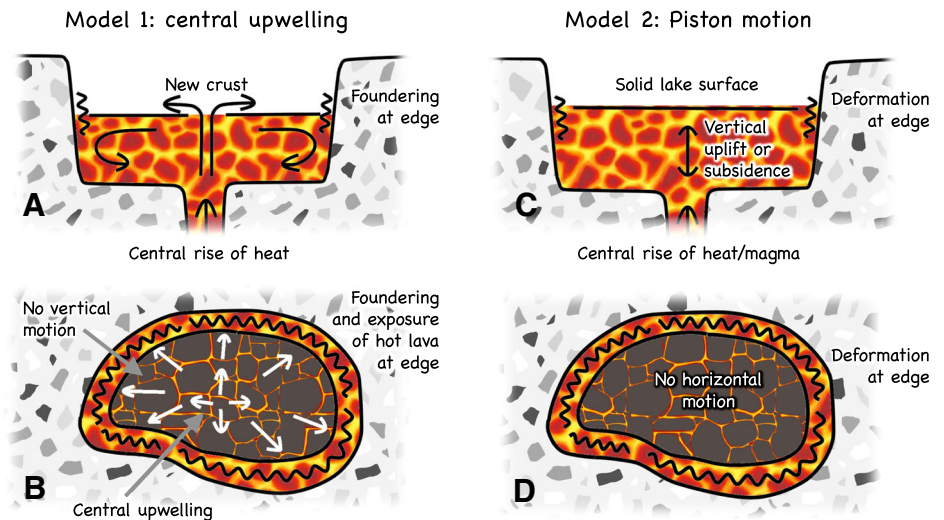
Discussion

Harris et al.¹⁹ and Harris²⁰ modeled the mass flux, heat loss and convection of several terrestrial lava lakes. In the case of Io, Lopes et al.² drew attention to a hypothetical cross-section of the Halema'uma'u lava lake in Hawai'i that was proposed by Perret²¹ in which there was a single circulation cell. We assert that such a single circulation cell within the lava lake would not produce the required foundering of the crust around the entire lake perimeter. Thus, we consider two different geologic models that might explain the thermal properties of these lava lakes (Fig. 6). In both models below, the bright lava ring around the perimeter of the lake would be produced by foundering/disrupting the lake surface to expose molten lava, which is inherently hotter than the crusted lake surface.

One possibility (Model 1, Fig. 6) is that there might be upwelling in the middle of the patera. The insulating crust (even a thin one, as per Oppenheimer and Yirgu²²) spreads radially via convection processes in the lake and then sinks at the edges, exposing lava. However, foundering of the lake crust at the walls does not necessarily produce spattering or exposure of molten lava. Also, we do not see any evidence of radial dependence of the radiance of the inner region (see Fig. 5, panel C). If the low radiance is interpreted as the residual heat from the magma that is shielded by the insulating crust, then such crust would have needed to maintain a uniform thickness while spreading radially.

Alternatively, a simple up-and-down "piston-type" movement of the entire lake surface (Model 2, Fig. 6) may cause disruption of the lava lake crust against the patera walls to reveal hotter material. For the piston-type lake model, the consistency between individual patera as well as the uniform

Fig. 6 | Two models for the motion of the lava lake surface and the resultant formation of the bright temperature rings. **A** Cross-section through a central upwelling (Model 1); **B** Plan view of central upwelling; **C** Cross-section through a piston motion model (Model 2); **D**: Plan view of the piston model.



brightness around the lake perimeter also poses geological challenges. Hot material would have to be exposed almost continuously for these bright rings to be produced, suggesting that vertical motion was ongoing at all sites. This in turn would imply that the lake levels might rise and fall enough that, at some sites, changes in the depth of the patera might be detected. No such depth changes at a specific patera have been reported, but the temporal and spatial resolutions of the images are indeed not sufficient to reveal vertical changes of less than several hundred meters.

The observation of activity at the borders of the lake raises the question of whether some type of thermal or mechanical erosion between the lake surface and the patera walls might be taking place. Potentially, this might imply that a patera increases in diameter over time, but less than a few hundred meters per year. In fact, in our observations, limited to 9 km/pixel resolution, we do not see any evidence for changes in size between observations by Voyager/Galileo and Juno. Radebaugh et al.³ identified a total of 417 paterae with a diameter range of 2.5 to 202.6 km, with a mean value of 41.0 km. If these paterae have similar origins, then the considered patera enlargement would imply that larger paterae are relatively old compared to the smaller ones. However, current data, both in terms of temporal and spatial resolution, do not allow us to draw a final conclusion on this.

In summary, our observations are compatible with a narrow zone of continuous spattering around the lake margin. Although the apparent annular width of these rings is in the 10–20 km range, based on thermal considerations we can argue that their physical width must be well below 1 km (see previous section). The diameters of these rings range between 50 and 100 km. While the maximum brightness observed by JIRAM in a lava ring depends on the observing geometry, combining multiple images acquired from different viewpoints allows us to safely determine that the patera is lower than the surrounding terrain and the patera's wall is quite steep, suggesting that the lava does not usually overflow the edge of the lake giving rise to substantial spills. All lava rings are quite narrow, as observed in few cases on Earth (see, for example, field photographs of the Kupaianaha lava lake at Kilauea volcano in Hawai'i—figure 15 in ref. 4, or the lava pond in the Pu'u 'Ō'ō crater, figure 10 in Heliker and Mattox²³). In contrast, a boiling lake without a substantial crust, such as Marum caldera in Ambrym Island²⁴, Vanuatu, would show thermal emission all over the patera rather than a ring near the edges.

Conclusions

The presence of infrared-bright rings surrounding the floors of numerous paterae on Io, as revealed by Juno/JIRAM, implies that this is a common process and a fundamental characteristic of eruptive activity within paterae.

These data are consistent with the observation of molten exposed lava at the edges of the paterae. Recycling of melt is implied by the lack of lava

flows on the rim of the paterae, indicating that there is a balance between melt that is erupted into the lava lakes and melt that is circulated back into the magmatic system. Several possible models for the ring formation are presented in this work in a preliminary way. Future studies should consider magma rise, containment within paterae, and tidal forcing as principal drivers for the formation of these unique features. Present findings highlight Io's abundant lava reserves, resembling lava lakes on Earth in some ways, yet distinctly different from any other phenomena observed in the Solar System.

Although Juno executed flybys of Io in December 2023 and February 2024, and more high-spatial resolution data of Io, in the visible or infrared, will be available before the end of the Juno mission, currently there are no planned missions that would acquire more data at similar spatial resolution. Once the last Juno data are acquired, examining visible images of inactive patera for signs of former lava lake activity would be instructive. The goal would be to identify features such as: (1) Vent structures that suggest former central upwelling; (2) Nested former lakes indicative of a late-stage reduction in magma production; and (3) Lava flows on the rim that indicate that the level of lava had risen to overtop the patera rim.

Data availability

The JIRAM dataset used for our analysis is publicly available at the Juno Archive at the Planetary Atmospheres Node (https://pds-atmospheres.nmsu.edu/PDS/data/PDS4/juno_jiram_bundle/data_calibrated/orbit51/).

Received: 23 February 2024; Accepted: 4 June 2024;

Published online: 20 June 2024

References

1. McEwen, A. S. et al. Galileo at Io: results from high-resolution imaging. *Science* **288**, 1193–1198 (2000).
2. Lopes, R. M. C. et al. Extraterrestrial lava lakes. *J. Volcanol. Geotherm. Res.* **366**, 74–95 (2018).
3. Radebaugh, J. et al. Patera on Io: a new type of volcanic caldera? *J. Geophys. Res.* **106**, 33,005–33,020 (2001).
4. Lopes, R., Spencer, J., Io after Galileo (Springer-Praxis, 2007).
5. Veeder, G. J. et al. Io: Heat flow from small volcanic features. *Icarus* **245**, 379–410 (2015).
6. Zambon, F. et al. Io hot spot distribution detected by Juno/JIRAM. *Geophys. Res. Lett.* **50**, e2022GL100597 (2023).
7. de Kleer, K., Rathbun, J. A., Io's thermal emission and heat flow. In *Io: A New View of Jupiter's Volcanic Moon* (eds. Lopes, R., de Kleer, K., Keane, J.) (Springer Nature, 2023).

8. Stansberry, J. A., Spencer, J. R., Howell, R. R., Dumas, C. & Vakili, D. Violent silicate volcanism on Io in 1996. *Geophys. Res. Lett.* **24**, 2455–2458 (1997).
9. McEwen, A. S. et al. High temperature silicate volcanism on Jupiter's moon Io. *Science* **281**, 87–90 (1998).
10. Allen, D. R., Radebaugh, J. & Stephens, D. C. Temperature and variability of Pillan, Wayland patera, and Loki Patera on Io from Cassini ISS data. *Icarus* **226**, 77–88 (2013).
11. Keszthelyi, L. P., Suer, T. A. The Composition of Io in *Io: A New View of Jupiter's Moon* (eds. Lopes, R. M. C., de Kleer, K., Tuttle Keane, J.), Astrophysics and Space Science Library, Vol 468 (Springer, 2023).
12. Lopes, R. et al. Lava lakes on Io. Observations of Io's volcanic activity from Galileo during the 2001 Fly-bys. *Icarus* **169**, 140–174 (2004).
13. McEwen, A. S., Keszthelyi, L., Lopes, R., Schenk, P., Spencer, J. The lithosphere and surface of Io. In *Jupiter: Planet, Satellites and Magnetosphere*, (eds. Bagenal, F., McKinnon, W., Dowling, T.) 307–328 (Cambridge Univ. Press, 2004).
14. Mura, A. et al. Infrared observations of Ganymede from Juno/Jovian infrared auroral mapper. *J. Geophys. Res. Planets* **125**, e2020JE006508 (2020).
15. Adriani, A. et al. JIRAM, the Jovian Infrared Auroral Mapper. *Space Sci. Rev.* **213**, 393–446 (2017). pages.
16. de Kleer, K. et al. Multi-phase volcanic resurfacing at Loki Patera on Io. *Nature* **545**, 199–202 (2017).
17. Williams, D. A. et al. Volcanism on Io: new insights from global geologic mapping. *Icarus* **214**, 91–112 (2011).
18. Ramsey, M. S., Chevrel, M. O., Coppola, D. & Harris, A. The influence of emissivity on the thermo-rheological modeling of the channelized lava flows at Tolbachik volcano. *Ann. Geophys.* **62**, VO222 (2019).
19. Harris, A. J. L. Modeling lava lake heat loss, rheology, and convection. *Geophys. Res. Lett.* **35**, L07303 (2008).
20. Harris, A. J. L., Flynn, L. P., Rothery, D. A., Oppenheimer, C. & Sherman, S. B. Mass flux measurements at active lava lakes: Implications for magma recycling. *J. Geophys. Res.* **104**, 7117–7136 (1999).
21. Perret, F. A. The circulatory system in the Halemau mau lava lake during the summer of 1911. *Am. J. Sci.* **35**, 337–349 (1913).
22. Oppenheimer, C. & Yirgu, G. Thermal imaging of an active lava lake: Erta 'Ale volcano, Ethiopia. *Int. J. Remote Sens.* **23**, 4777–4782 (2002).
23. Heliker, C. & Mattox, T. N. The first two decades of the Pu'u 'O'o-Kupaianaha eruption: chronology and selected bibliography. *U.S. Geol. Surv. Profess. Pap.* **1676**, 1–28 (2003).
24. Radebaugh, J., Lopes, R. M., Howell, R. R., Lorenz, R. D. & Turtle, E. P. Eruptive behavior of the Marum/Mbwelesu lava lake, Vanuatu and comparisons with lava lakes on Earth and Io, J. *Volcanol. Geotherm. Res.* **322**, 105–118 (2016).

Acknowledgements

We thank Jani Radebaugh and Christopher Hamilton for providing insightful comments and suggestions which greatly improve the value of this work. We also thank Agenzia Spaziale Italiana (ASI) for the support of the JIRAM contribution to the Juno mission. This work is funded by the ASI-INAF Addendum no. 2016-23-H.3-2023 to grant 2016-23-H.0.

Author contributions

A.Mu, F.T., F.Z., R.M.C.L., J.R., H.B., S.B. and C.J.H. conceived the study. S.B., A.A., G.F., G.S. and G.P. designed the experiment. G.F., G.S. and A.Mu. performed the instrument calibrations. A.M. and F.T. performed the geometry reconstruction. R.S. and A.C. managed the operation of the JIRAM instrument. R.N. was responsible for the JIRAM calibration pipeline. A.Mu analyzed the data and made plots, writing major sections of the main text. R.M.C.L. and P.J.M.M. contributed to the initial draft; F.T., F.Z., J.R., C.J.H. and H.B. revised the initial draft. A.Mu., F.T., FZ, R.M.C.L., P.J.M.M., H.B., G.F., A.Mi., C.J.H., A.A., F.A., S.B., E.D.M., D.G., A.Mo., M.P., G.P., C.P., J.R. and G.S. contributed to revision of the manuscript. All authors discussed the results and commented on the manuscript.

Competing interests

The authors declare no competing interests.

Additional information

Supplementary information The online version contains supplementary material available at <https://doi.org/10.1038/s43247-024-01486-5>.

Correspondence and requests for materials should be addressed to Alessandro Mura.

Peer review information *Communications Earth & Environment* thanks Jani Radebaugh and the other, anonymous, reviewer(s) for their contribution to the peer review of this work. Primary Handling Editor: Joe Aslin. A peer review file is available.

Reprints and permissions information is available at <http://www.nature.com/reprints>

Publisher's note Springer Nature remains neutral with regard to jurisdictional claims in published maps and institutional affiliations.

Open Access This article is licensed under a Creative Commons Attribution 4.0 International License, which permits use, sharing, adaptation, distribution and reproduction in any medium or format, as long as you give appropriate credit to the original author(s) and the source, provide a link to the Creative Commons licence, and indicate if changes were made. The images or other third party material in this article are included in the article's Creative Commons licence, unless indicated otherwise in a credit line to the material. If material is not included in the article's Creative Commons licence and your intended use is not permitted by statutory regulation or exceeds the permitted use, you will need to obtain permission directly from the copyright holder. To view a copy of this licence, visit <http://creativecommons.org/licenses/by/4.0/>.

© The Author(s) 2024